

Static Modelling, Automation and Control of PRR Parallel Manipulator

Ganesh Mangavu*, P. Kalyan Kaushik, Utsav Ranjan, R. Shyam, N. S. Mithun and Anjan Kumar Dash

School of Mechanical Engineering, SASTRA University, Thanjavur - 613401, Tamil Nadu, India; ganeshm@mech.sastra.edu, Pkalyan91@gmail.com, utsav24ranjan@gmail.com, shyamram66@gmail.com, nsmithun94@gmail.com

Abstract

Background/Objectives: Parallel manipulators edge over serial manipulators for their performance characteristics such as high accuracy and low inertia. In this paper, PRR planar parallel manipulator with elevated links was studied and analyzed. **Methods/Statistical Analysis:** Kinematic simulation was carried out and the workspace of the manipulator was determined. Static analysis including stress analysis, torque and inertia computations was made. Stress analysis of manipulator was done by ANSYS. **Findings:** Simple analytical method was employed for finding workspace area. The load bearing capability of the non planar links was high compared to the planar links. The inertia computations of the lead screw and the inclined links provide promising results for system dynamics. **Application/Improvements:** Non-planar links will be useful for manipulators facing challenges in dynamics.

Keywords: Moment of Inertia, Non-Planar Links, Planar Parallel Manipulator, Stiffness, Stress Analysis

1. Introduction

A parallel manipulator is a closed loop kinematic mechanism with a minimum of two kinematic chains linking the base platform and the end-effectors. The mobile platform is movable with respect to the base platform. In general, the parallel manipulator with 'n' degrees of freedom is actuated by 'n' actuators merlet¹. Parallel manipulators provide higher strength/weight, stiffness/weight ratios and precise positioning than serial manipulators. Moreover, parallel manipulators allow the actuators to be fixed to the base or to be located close to the base of the mechanisms², which minimizes the inertia of the moving parts and makes it possible to use more powerful actuators. Three legged planar manipulators are noted for its low inertia. They also have less leg interference, due to the presence of fewer legs in comparison to the six legged manipulators.

The last two decades have witnessed considerable research in parallel manipulators. The research efforts include

inverse position kinematics, direct position kinematics, singularities, workspace and dexterity, and dynamics and control³ etc. Inverse Kinematics was solved using algebraic method^{4,5}. The types of singularities were discussed in⁶ and⁷. Polynomial describing the singularity loci was reduced from higher order to lower order⁸. Determination of workspace for 3-DOF manipulators was elaborated in⁹. The work reported by Masory and Wang¹⁰ determined workspace sections for various configurations with the constraints such as joint angle limits and leg interference. Gosselin¹¹ optimized the design of 3-DOF manipulators by maximizing workspace and dexterity. Multi-objective optimization was done by Chablat¹² for a constrained workspace.

In case of traditional 3-PRR planar manipulator, all the proximal links and the distal links are in a common horizontal plane. Due to this, the links are subjected to cantilever action and it limits the load carrying capacity of the parallel manipulator. The same planar manipulator with inclined links reduces the cantilever action and

*Author for correspondence

increases the overall stiffness. Hence the inertia property and accuracy/stiffness are enhanced.

In this paper, the static analysis of the model is studied and analysed. The purpose of the analysis is also to substantiate the improved performance of the static characteristics such as stress and inertia. A prototype was fabricated to perform experimental tests. The prototype was constructed by aluminium links and lead screws for linear actuation. MSP430g2553 microcontroller was used to control the motors. Communication between user interface and microcontroller is by serial communication (UART Protocol).

2. Inverse Kinematic Analysis

The inverse kinematics for this manipulator gives the distance to be moved by the slider of prismatic joint and

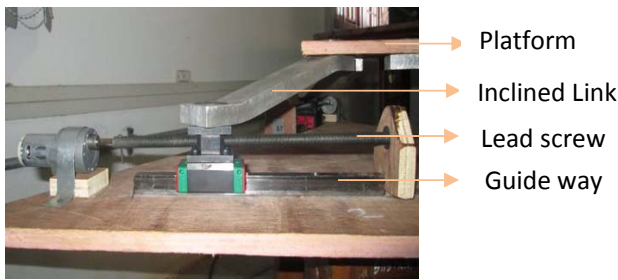


Figure 1. 3D model of PRR manipulator with non planar links. The links connected to the base actuator is inclined in vertical direction with respect to horizontal direction by 30 degree.

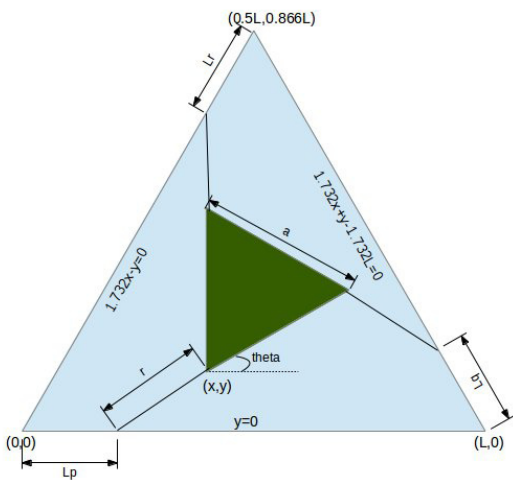


Figure 2. 3-PRR planar Parallel Manipulator.

hence control the PRR manipulator to reach the position as entered by the user.

Figure 2 is a simple geometrical representation of the parallel manipulator. Both the base and top triangles are equilateral with dimensions $L = 540\text{mm}$ and $a = 94\text{mm}$ respectively. The rotary link denoted by $r (= 186\text{mm})$ joins the base and top triangle by two rotary joints. L_p, L_q, L_r are the distances moved by the slider of prismatic joints along the sides of base triangle. We get the equation of edges of base triangle as $y = 0, 1.732x + y - 1.732L = 0$ and $1.732x - y = 0$ respectively.

Let us consider finding out L_p . It can be extended similarly to find L_q and L_r respectively (Figure 3).

We know co-ordinates of A(origin) and D(entered by the user).

$$AD = \sqrt{y^2 + x^2}; CD = r \quad (1)$$

$$BC = \sqrt{CD^2 + BD^2} \text{ or } BC = \sqrt{CD^2 - BD^2} \quad (2)$$

(for two possible orientations)

$$\text{Similarly, } L_p = AB - BC \text{ or } L_p = AB + BC \quad (3)$$

$$BC' = \sqrt{C'D^2 + BD^2} \quad (4)$$

The other two vertices of the top platform are found with the help of $(x, y), \theta$ and α .

Vertices coordinates are

$$x + a \cos(\theta), y + a \sin(\theta), (x + a \cos(\theta + \pi/3))$$

$$\text{and } y + a \sin(\theta + \pi/3) \quad (5)$$

Similarly, the procedure is repeated for L_q and L_r respectively.

3. Workspace

The length of slider joint is taken equal to the side length of base triangle depending upon the size of the top platform,

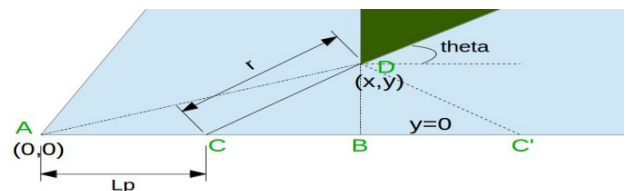


Figure 3. Schematic of one leg.

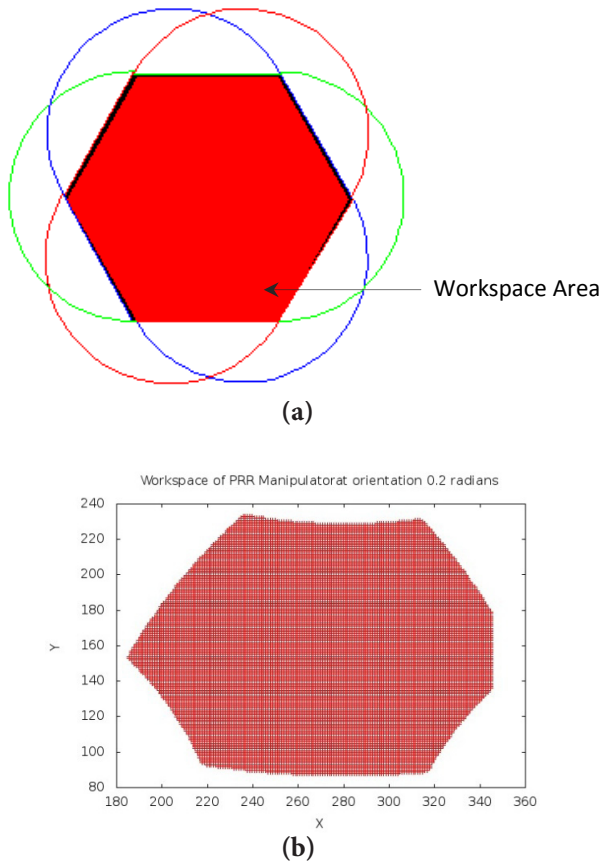


Figure 4. (a) Hexagonal workspace area. For various combinations of geometric parameters, different workspace shapes are possible. Of which hexagonal workspace provides a sizeable area. (b) Workspace for 0.2 radian Top platform orientation.

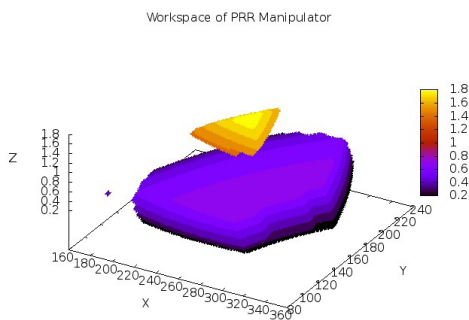


Figure 5. Workspace generated for different orientations of the Top platform.

valid workspace is created i.e., only when the radius of the top $L_p = L_{B\Delta}$ platform is within certain range. Otherwise there is null workspace. The workspace area takes the form of inverted triangle with its vertex downwards or an hexagonal area.

4. Formulation of Inertia Tensor

The moment of inertia and inertia tensor is determined for performing the stiffness analysis by Matrix Structural method because the links are assumed as 3D spring models

Assuming the link as a 3D spring model, the compliance matrix for the link element is

$$\frac{1}{E} \begin{bmatrix} L/A & 0 & 0 & 0 & 0 & 0 \\ 0 & 1/3I_z L & 0 & 0 & 0 & -1/2I_z \\ 0 & 0 & 1/3I_y L & 0 & -1/2I_y & 0 \\ 0 & 0 & 0 & \frac{E.L}{G.J} & 0 & 0 \\ 0 & 0 & -1/2I_y & 0 & L/I_y & 0 \\ 0 & 1/2I_z & 0 & 0 & 0 & L/I_z \end{bmatrix}$$

where, E is the young's modulus, L is the length of the link, I is the second moment of area, G is the Coulomb modulus and A is the area of cross section.

In the matrix elements, cross section area A and inertia I will be corresponding to the cross section area given by Equation (7).

Let us consider a link of cross section area bw and length L inclined in XZ- plane. In order to determine the moment of inertia (second moment of area) about the Z-axis, the cross section area of the inclined link in the X-Y plane is considered.

$$\text{Area of cross section } A = bh = \frac{bw}{\sin \delta} \tag{7}$$

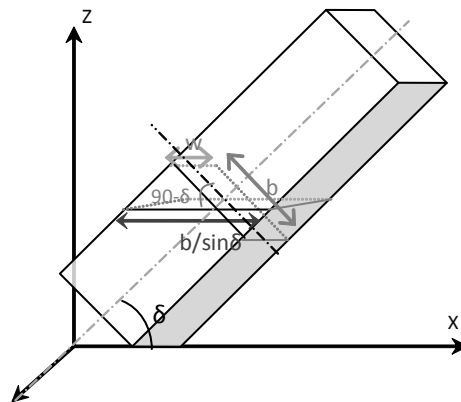


Figure 6. A link in XZ plane with an inclination angle of δ . The cross section area of the link in XY plane is $bw/\sin \delta$ compared to original cross section area bw . This area is used for computing the moment of inertia.

Second moment of Area

$$I_x = \iint_A y^2 dydx = \frac{b^3 w}{12 \sin \delta} \tag{8}$$

Second moment of Area

$$I_y = \iint_A x^2 dx dy = \frac{b}{12} \left(\frac{w}{\sin \delta} \right)^3$$

Polar moment of inertia

$$I_z = I_y + I_x = \frac{1}{12} \left[\left(\frac{b^3 w}{\sin \delta} \right) + b \left(\frac{w}{\sin \delta} \right)^3 \right] \tag{9}$$

Due to the presence of $\sin \delta$ term in Equation (8) and Equation (9), moment of inertia increases nonlinearly with δ . With the rise in moment of inertia, the compliance of the links is very much reduced in comparison to the links of planar legs.

5. ANSYS Stress Analysis

Methodology:

This modified design is analysed using ANSYS Workbench for Static Structural analysis.

The following procedure was followed:

1. Building the model in Pro-E.
2. Entering the necessary data.
3. Importing the Pro-E model in ANSYS.
4. Meshing of the model involving triangular meshes.
5. Applying the loads and 6. Solving and plotting the results.

For the base, table and the lead screw, material selected is Steel and for all other components Aluminium alloy is selected. The material properties are listed in the following Table 1.

The model is meshed using mesh tool. A 3 kg of load is distributed uniformly over the surface of top table. In this analysis, deformation plot and stress plots are determined for equivalent stress (Von-Mises) theory, maximum normal stress theory and maximum principal stress theory.

Table 1. Material Property

Properties	Aluminium Alloy	Steel
Young's modulus	71000 MPa	200000 MPa
Density	2.77e-06 kg/mm3	7.85e-06 kg/mm3
Poisson's ratio	0.33	0.30
Yield strength	280 MPa	250 MPa
Ultimate strength	310 MPa	460 MPa

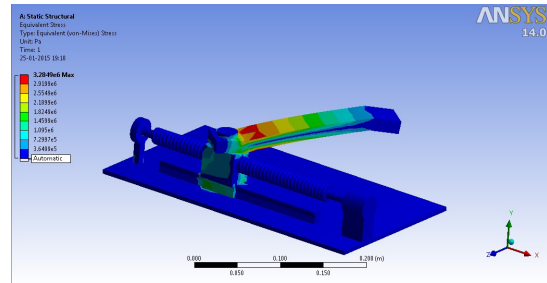


Figure 7. Stress analysis.

Table 2. Stress analysis results

Static analysis	Theoretical
Maximum Equivalent Stress (Von Mises)	17.8MPa
Maximum Normal Stress	18.6MPa
Maximum Principal Stress	18.6MPa
Maximum Deflection under Static Loading	0.0102 m

6. Automation and Control

The co-ordinate of one of the top platform vertex and orientation of end effector is provided to the computer interface. In accordance with inverse kinematics, length to be traversed by each prismatic joint is calculated. Ultrasonic Sensor HCSR04 senses the current position of the prismatic joint. The difference between the actual position of slider (prismatic joint) and the expected position is calibrated. It can be either positive or negative. For the end effector to be at desired position and orientation, slider might have to go forward or backward. The distance to be moved is converted into time for which motor has to be turned on. This is done in accordance with speed of the motor and pitch of the lead screw. The motor is rotated in requisite direction for requisite time with the help of L293d motor driver IC. The sensor again checks the position of the prismatic joint and if there is more than tolerable discrepancy in its position, then the calibration steps are repeated again.

The above process is coordinated and controlled using MSP430g2553 microcontroller. The communication between user at computer and MSP430 is through USB cable which is then converted to UART protocol by FTDI chip in MSP430 controller board circuit.

7. Conclusion

The 3-PRR non-planar parallel manipulator is fabricated as per the design. It is coordinated and controlled using

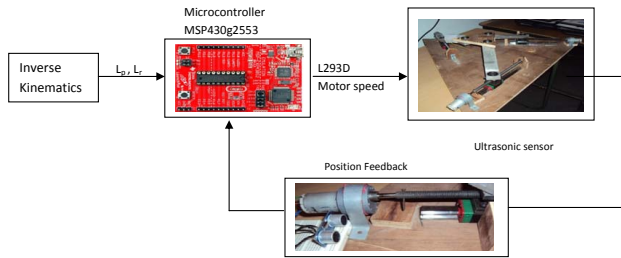


Figure 8. Automation and control of proposed PRR manipulator.

MSP430g2553 microcontroller. This manipulator was designed to show the improved performance of non-planar links ahead of planar links. Considerable workspace is achieved for the dimensions chosen. The load carrying capacity, inertia and stiffness of the manipulator showed promising results. This is proven through inertia computations, torque calculations and ANSYS workbench results.

8. References

1. Merlet JP. Direct kinematics of planar parallel manipulators. *Proceedings of IEEE International Conference on Robotics and Automation*. 1996; 4:3744–9.
2. Zhang X. Dynamic modeling and active vibration control of a planar 3-PRR parallel manipulator with three flexible links [PhD thesis]. University of Toronto; 2009.
3. Bonev IA. Design and analysis of 6-Dof 6-PRRS parallel manipulators [PhD thesis]. Department of Mechatronics, Kwangju Institute of Science and Technology; 1998.
4. Williams II RL, Shelley BH. Inverse kinematics for planar parallel manipulators. *Proceedings of DETC '97 ASME Design Technical Conferences*; Sacramento, California. 1997. p. 1–6.
5. Pennock GR, Kassner DJ. Kinematic analysis of a planar eight-bar linkage: Application to a platform-type robot. *ASME Mechanisms Conference*. 1990. DE-25:37–43.
6. Bonev IA, Gosselin CM. Singularity loci of planar parallel manipulators with revolute joints. *Proceedings of 2nd workshop on computational kinematics*; Seoul, South Korea. 2001. p. 1–9.
7. Daniali HRM, Zsomer-Murray PJZ, Angeles J. Singularity analysis of planar parallel manipulators. *Mechanism and Machine Theory*. 1995; 30(5):665–78.
8. Firmani F, Podhorodeski RP. Singularity analysis of parallel manipulators based on forward kinematic solutions. *Mechanism and Machine Theory*. 2009; 44(7):1386–9.
9. Merlet J-P, Gosselin CM, Mouly N. Workspace of planar parallel manipulators. *Mechanism and Machine Theory*. 1998; 33(1–2):7–20.
10. Masory O, Wang J. Workspace evaluation of Stewart platform. *Advanced Robotics*. 1995; 9(4):443–61.
11. Gosselin CM, Angeles J. The optimum kinematic design of a planar three-degree-of freedom parallel manipulator. *ASME Journal of Mechanisms, Transmission and Automation in Design*. 1988; 110(1):35–41.
12. Chablat D, Caro S, Ur-Rehman R, Wenger P. Comparison of planar parallel manipulator architectures based on a multi-objective design optimization approach. *34th Annual Mechanisms and Robotics Conference (MR)*; Montreal, Canada. 2010. p. 861–70.